Progress In Electromagnetics Research, PIER 41, 133–157, 2003

NUMERICAL STUDIES OF METALLIC PBG STRUCTURES

A-C. Tarot, S. Collardey, and K. Mahdjoubi

Institut d'Electronique et Télécommunications de Rennes (IETR)
Groupe Antennes et Hyperfréquences
UMR CNRS 6164
Université de Rennes I
Bât 11 D - Campus de Beaulieu
Avenue du Général Leclerc
35042 Rennes Cedex, France

Abstract—Photonic Bandgap (PBG) materials have been investigated for their versatility in controlling the propagation of electromagnetic waves [1, 2]. In order to determine PBG structures responses, several analytical or numerical methods are used, such as:

- The plane wave method applied to solve Maxwell's equations [3].
- The transfer matrix method, based on the wire grating impedance developed by N. Marcuvitz [4].
- The Finite Element Method (FEM) exhibits, e.g., the frequency response of reflection and transmission coefficients of the PBG materials when they have infinite surfaces and are excited by plane wave. The FEM method can be also used in the case of finite structure fed by a dipole.
- The Finite Difference Time Domain method (FDTD). This method solves the discretized Maxwell's equations in the time domain and evaluates the electromagnetic field components. These EM fields are then obtained in the frequency domain thanks to a Fourier Transform.

First of all, we present a parametrical study using a 3D Finite Element method software. This study allows to estimate the role of any parameters on the reflection and transmission coefficients and then to design a PBG structure in the X-band (8–12 GHz). Continuous and discontinuous structures are presented.

Then, we present a numerical analysis of PBG structures, using the FDTD method in order to understand the propagation phenomena in these periodic materials.

1. PARAMETRICAL STUDY IN X-BAND WITH THE 3D FINITE ELEMENT METHOD

1.1. Introduction

The PBG materials are characterized by the period between two elements of the structure, the diameter of metallic wires and the number of layers. A PBG structure presents a succession of stop-bands and propagation bands which depend on its physical parameters as well as the wave incidence, the dielectric permittivity.... The purpose of this part is to study these parameters influence on reflection (S_{11}) and transmission (S_{21}) coefficients.

This study is purely theoretical. All simulations have been realized with Ansoft HFSS Software [5] and an add-on module OPTIMETRICS. HFSS is a 3D electromagnetic simulation software that computes S-parameters and full-wave fields for arbitrarily-shaped 3D passive structures. OPTIMETRICS performs parametric analysis, sensitivity analysis and optimization. Infinite periodic structures (in y and z directions) are realized using PEC (Perfect Electrical Conductor) and PMC (Perfect Magnetic Conductor) boundary conditions and

excited with a normal incident plane wave. MATLAB Software is used to visualize the reflection and transmission coefficients. The abbreviations used in this chapter are listed below:

p_t: transverse period

p_l: longitudinal period (along the direction of propagation)

d: diameter of metallic wire

n: number of layers

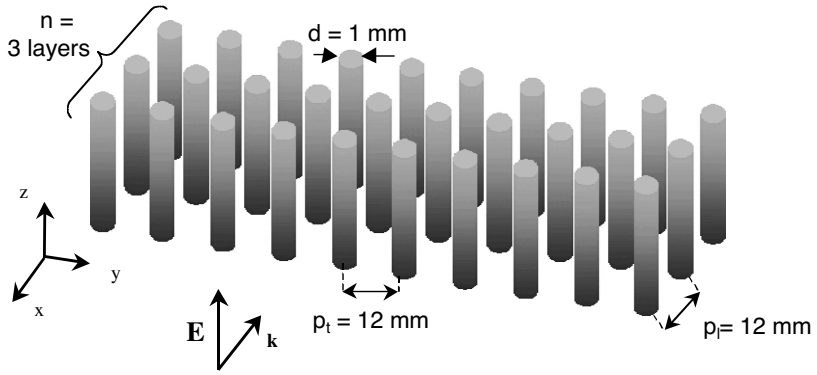

Figure 1. Geometry of a 2-D square lattice metallic PBG with 3 layer, a 12 mm period ($p_l = p_t$) and a 1 mm diameter.

1.2. Review on Metallic PBG Structure of Continuous Wires

Let us consider the simple 2-D square lattice metallic PBG described in Figure 1. It is composed of 3 layers with a 12 mm period and metallic wires with a diameter of 1 mm. This structure is supposed infinite in y and z directions. When this structure is excited by a normal incident plane wave, with the electric field parallel to the wires' axis, this kind of structure exhibits a bandgap (high reflection level) starting from 0 Hz to 7.5 GHz, the cutoff frequency which depends on PBG physical parameters. Then, there is a propagation band (low reflection level) composed of 2 propagation peaks and finally a second stopband. We can recall there are $(N-1)$ Fabry-Perrot cavities in a N layer structure and then $(N-1)$ resonance frequencies associated. Therefore the number of these propagation peaks (N_{peaks}) is linked up the number of layers (N_{layers}) with the following relationship (valid only for normal incidence):

$$N_{peaks} = N_{layers} - 1 \tag{1}$$

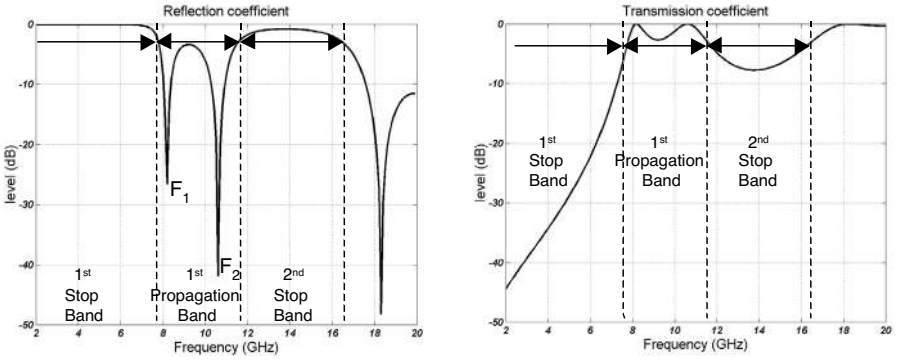

(a) (b)

Figure 2. Theoretical reflection S_{11} (a) and transmission S_{21} (b) coefficients of the metallic PBG structure described in Figure 1 (3 layers, $p_l = p_t = 12\,\text{mm}$, $d = 1\,\text{mm}$).

Table 1. Parametric study of a continuous PBG structure.

p_l (mm)	p_t (mm)	d (mm)	n	ε_r	Figure
9 to 15	12	1	3	1	Figure 3
12	9 to 15	1	3	1	Figure 4
12	12	0.5 to 1.5	3	1	Figure 5
12	12	1	3 to 5	1	Figure 6
12	12	1	3	1 to 10	Figure 7

1.2.1. Influence of Period, Diameter, Number of Layers and Permittivity

We are interested in studying a metallic PBG structure, which allows the propagation in the X-band. Dimensions of such a structure were previously mentioned: $p_l = p_t = 12\,\text{mm}$, $d = 1\,\text{mm}$, $n = 3$ layers. We vary each parameter around these reference values, and also the dielectric permittivity. All these variations and corresponding figures are listed in the Table 1.

- When longitudinal period increases (Figure 3), propagation peak frequencies (F_1 and F_2) decrease as well as the propagation bandwidth and stop bandwidth. The same phenomenon is observed with the dielectric permittivity (Figure 7).
- When transverse period increases (Figure 4), stop band and propagation band frequencies decrease whereas bandwidth between propagation peaks grows up slightly.

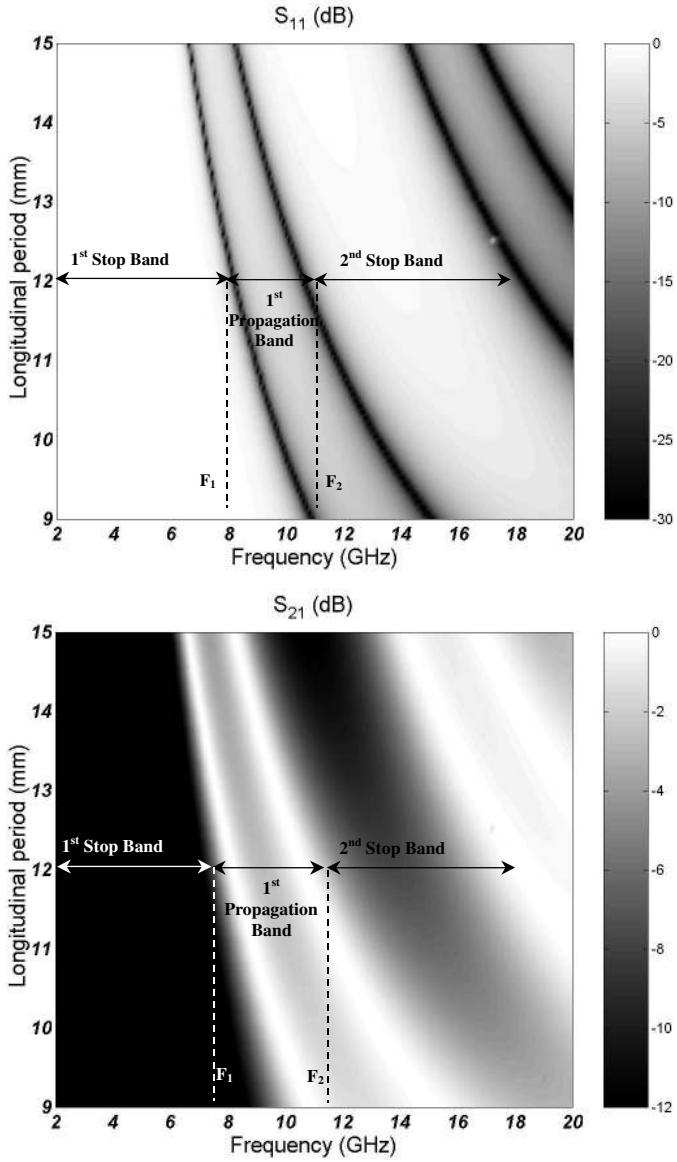

Figure 3. Longitudinal period influence on reflection (S_{11}) and transmission (S_{21}) coefficients.

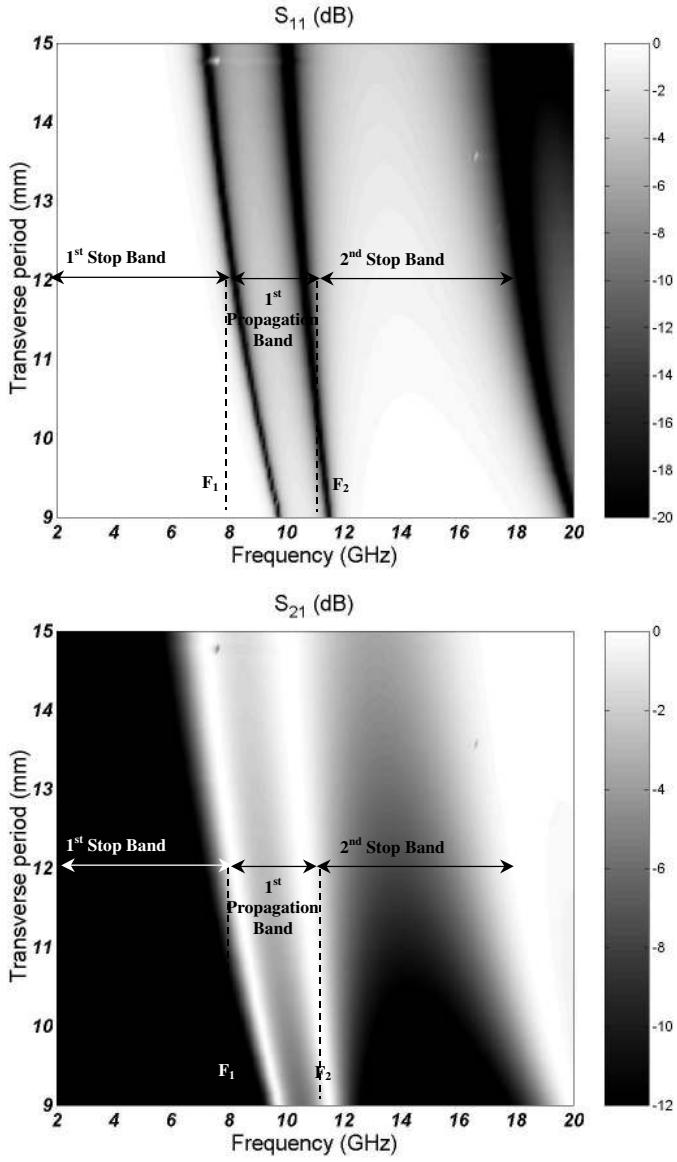

Figure 4. Transverse period influence on reflection (S_{11}) and transmission (S_{21}) coefficients) coefficients.

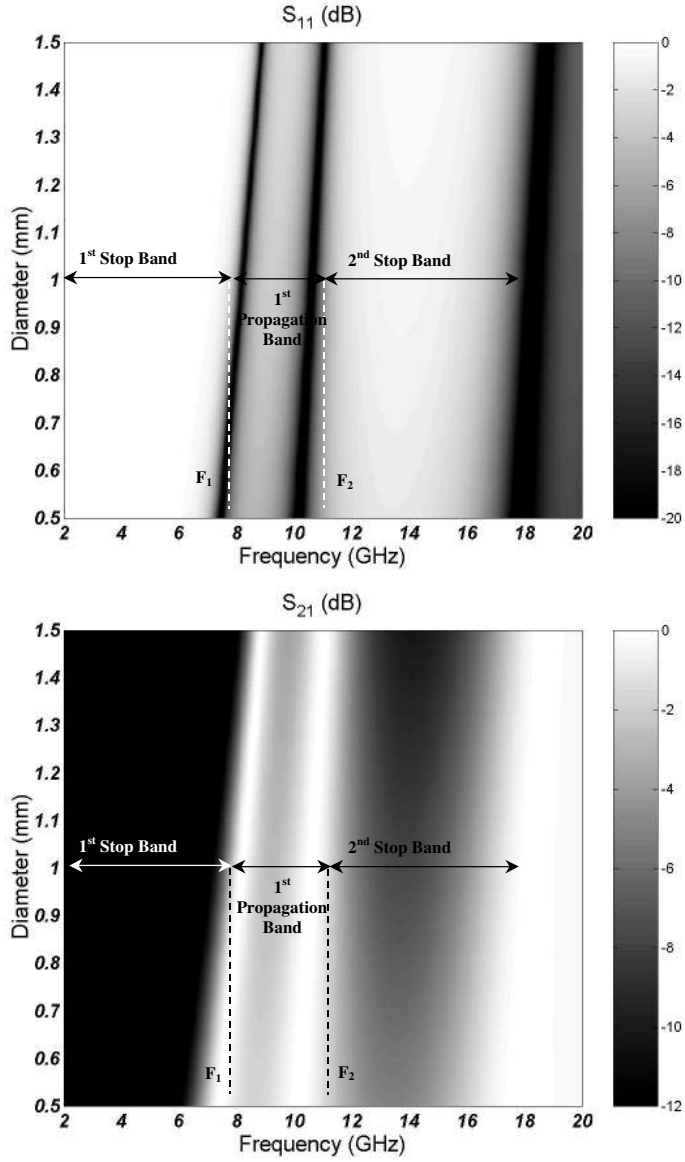

Figure 5. Diameter influence on reflection (S_{11}) and transmission (S_{21}) coefficients.

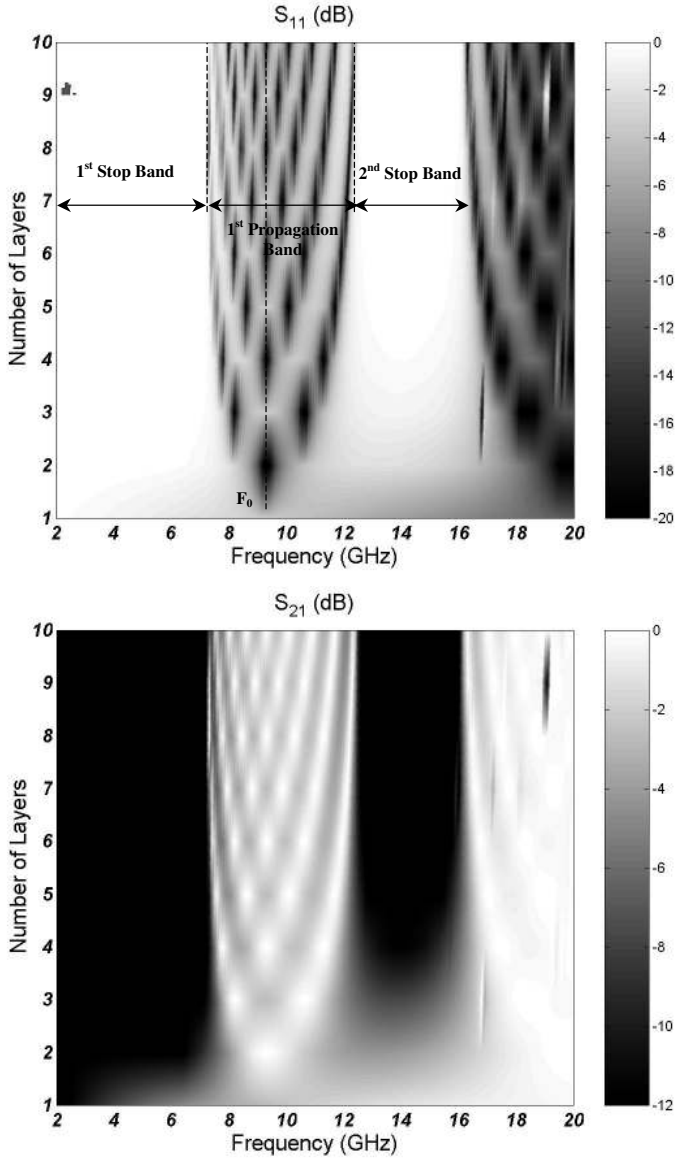

Figure 6. Number of layers influence on reflection (S_{11}) and transmission (S_{21}) coefficients.

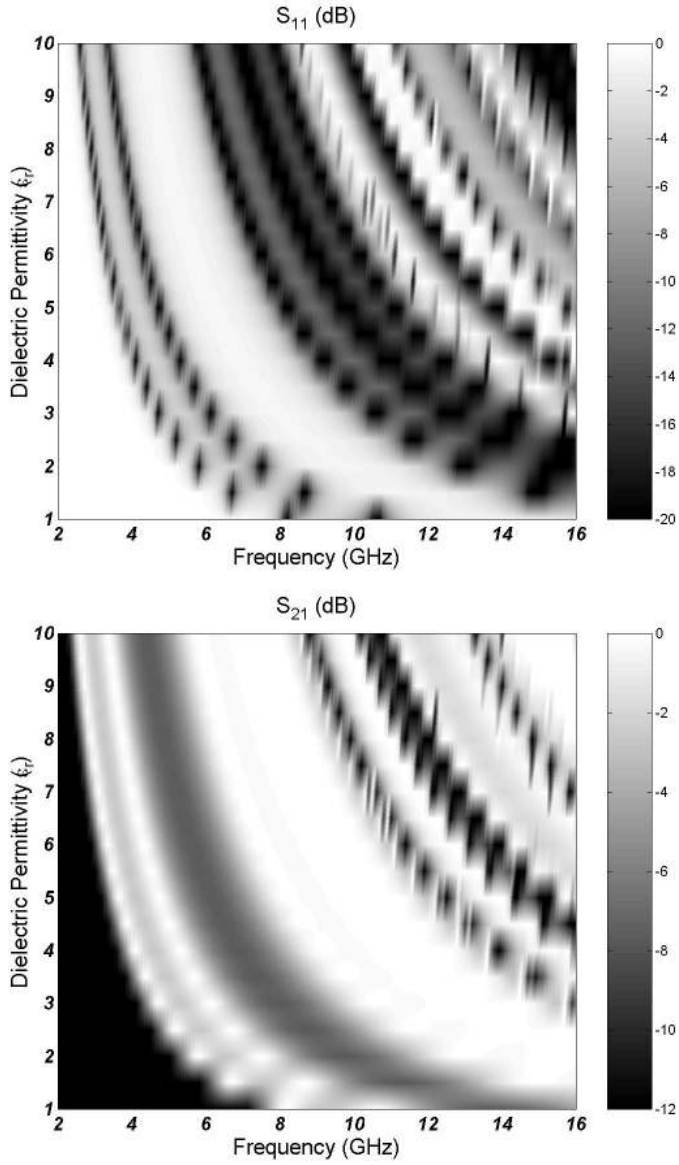

Figure 7. Permittivity influence on reflection (S_{11}) and transmission (S_{21}) coefficients.

- On the other hand, the *diameter* of wires (Figure 5) and the propagation peaks increase in the same time, whereas the propagation bandwidth decreases.
- For a n *layers* structure (Figure 6), we can verify there are $(n-1)$ propagation peaks. It is interesting to notice that the propagation bandwidth increases until $n = 7$ layers, and then remains constant. Moreover the central peak (f_0) is the same regardless of the number of layers.

Moreover, we can notice that a low longitudinal period, a high transverse period, a thin diameter and a low number of layers are suitable to improve the propagation (that is to perform a high transmission coefficient).

In the Table 2, we summarize the influence of each parameter on all the propagation frequencies (F_1 and F_2), the propagation bandwidth and the stop bandwidth.

Table 2. Parameters influence on the propagation and stop bands.

Parameter	Propagation peaks F_1 et F_2	Propagation Bandwidth	Stop Bandwidth	magn (S21) in the StopBand
pl ↗	↘	↘	↘	↘
pt ↗	↘	↗	↘	↗
d ↗	↗	↘	↗	↘
n ↗	(n-1) propagation peaks	↗ until n=7	↘ until n=7	↘
er ↗	↘	↘	↘	no effect

1.3. Review on Metallic PBG Structure of Discontinuous Wires

We now consider the metallic PBG structure described in Figure 8. It is composed of three layers of discontinuous wires. Besides the previous abbreviations (n, d, p_l, p_t), the axial period (p_z) and the spacing (e) are used. From the transmission coefficient (Figure 9), we can notice that the structure of discontinuous wires exhibits a propagation band from 0 Hz to about 8 GHz and then a stop band and a propagation band. The metallic PBG of discontinuous wires has the same behavior as the dielectric PBG [6, 7]. The interest of such a structure is to introduce active components (like Field Effect Transistor [8] or PIN Diode [9]) in the spacing and then to switch from a propagation band to a stop band.

If we consider a discontinuous metallic PBG structure allowing the transmission in the X-band, the news dimensions are then: $p_l = p_t = 7$ mm, $p_z = 5$ mm, $e = 1$ mm, $d = 1$ mm and $n = 3$ layers.

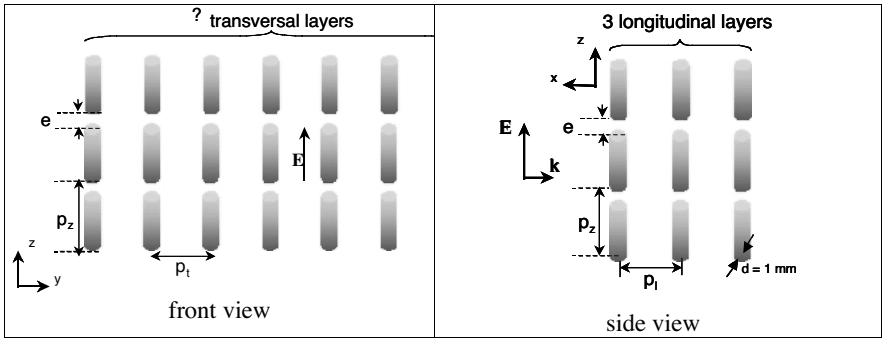

Figure 8. Geometry of a discontinuous PBG structure.

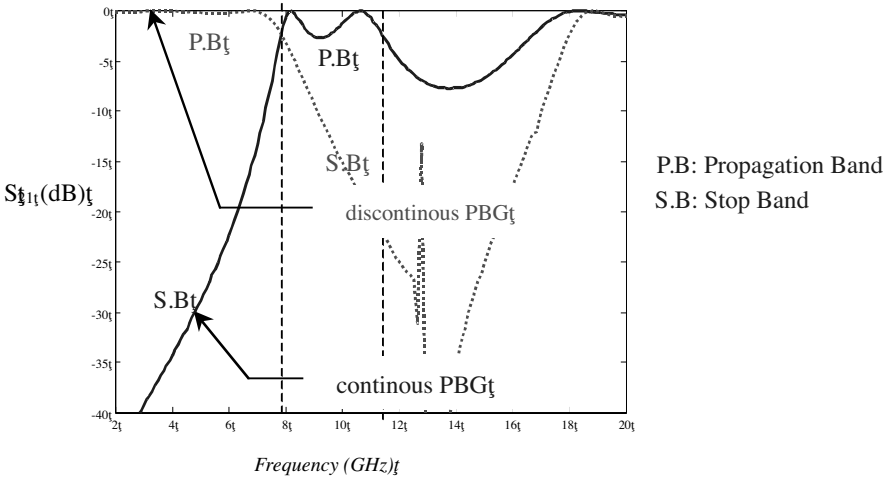

Figure 9. Transmission coefficient of the continuous and discontinuous metallic PBG structure with $n = 3$ layers, $d = 1$ mm, $p_l = p_t = 12$ mm, $-p_z = 12$ mm and $e = 2$ mm for the discontinuous PBG.

1.3.1. Influence of Transverse Period (p_t), Axial Period (p_z) and Spacing (e)

A variation of the transverse period (p_t), the axial period (p_z) and the spacing (e) are realized round their reference values (cf Table 3). The other parameters (p_l, d, n, ε_r) exhibit the same evolution that those of a continuous metallic PBG.

The influence of each parameter is summarized in the Table 4.

Table 3. Parametric study of a discontinuous PBG structure.

pl (mm)	p_t (mm)	p_z (mm)	e (mm)	d (mm)	ε_r	Figure
7	5 to 9	5	1	1	1	Figure 11
7	7	5 to 9	1	1	1	Figure 12
7	7	5	0.5 to 4	1	1	Figure 13

Table 4. Parameters influence on the propagation and stop bands.

Parameter	Propagation Bandwidth	Stop Bandwidth
p_t ↗	no effect	no effect
p_z ↗	↘	↗
e ↗	↗	↘

Because of a great number of parameters, it's more difficult to design a discontinuous metallic PGB structure. A solution is to conceive a continuous structure in adjusting correctly its parameters $(p_l, p_t, d, n, \varepsilon_r)$ in order to present a dual transmission coefficient (that is a P.B if a S.B is required and inversely). And then, the axial period (p_z) and the spacing (e) are still to be adjusted.

2. MODAL ANALYSIS OF MPBG WITH THE FDTD METHOD

2.1. Introduction

As seen before, different techniques can characterize infinite photonic band-gap structures. But the PBG have finite dimensions and it becomes more difficult to determine modal characteristics (reflection or transmission coefficients, radiation pattern...). So, we use the FDTD method (Finite-Difference Time-Domain) [10, 11] to these structures to obtain such characteristics and also the propagation modes inside or outside the PBG, when it is associated with the Fourier transform. The method based on the FDTD and the Fourier transform is described. This method has been already applied with success to the dielectric PBG materials [12] where the propagation wave vectors of the infinite structure are compared with these of the finite structure. So, we only present results obtained with the metallic PBG materials.

We explain, how to visualize the propagation wave vector of a finite periodic structure in the reciprocal space thanks to the time or

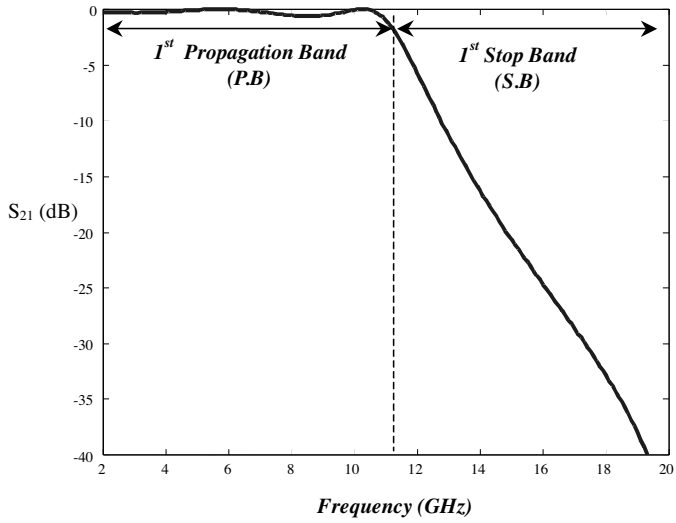

Figure 10. Theoretical transmission coefficient (S_{21}) of the discontinuous metallic PBG structure with $n = 3$ layers, $d = 1\,\text{mm}$, $p_l = p_t = 7\,\text{mm}$, $p_z = 5\,\text{mm}$ and $e = 1\,\text{mm}$.

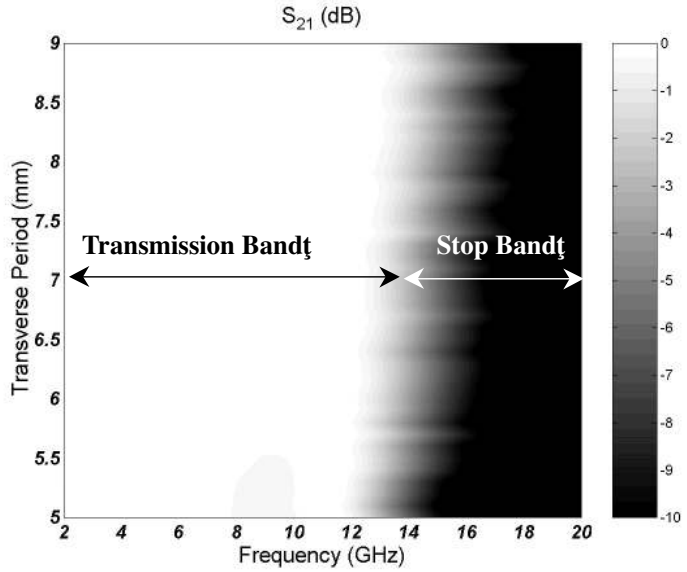

Figure 11. Transverse period (p_t) influence on transmission coefficient (S_{21}).

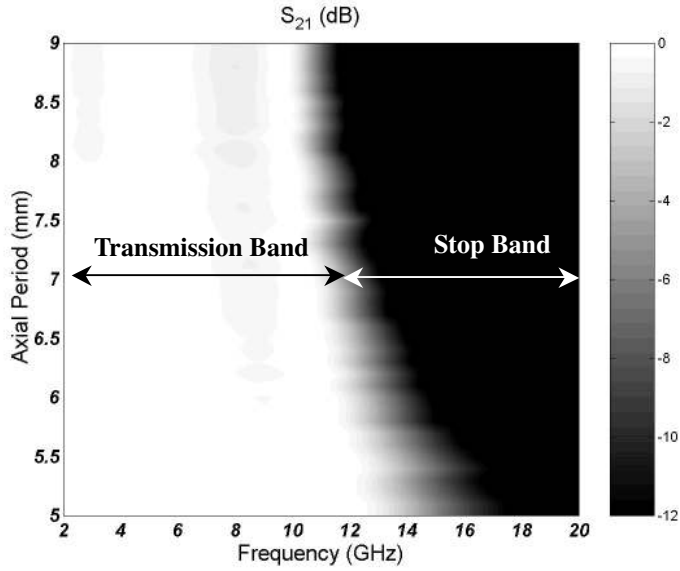

Figure 12. Axial period (p_z) influence on transmission coefficient (S_{21}).

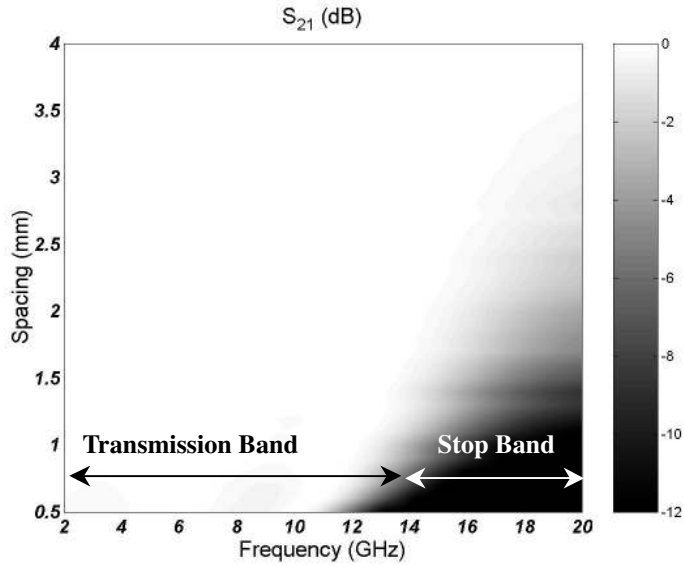

Figure 13. Spacing (e) influence on transmission coefficient (S_{21}).

frequency domain electromagnetic (EM) fields components [13]. This numerical technique can be implemented easily if we have an EM simulator and a visualization software. The method is widely described and finally, we present some results to show the propagation modes.

2.2. The Analysis Method

Based on the FDTD method and the Fourier transform in time and space domain, this method allows to visualize propagation modes in the reciprocal space (or wave vector space). The comparison between the mode repartition in the k-space and the radiation pattern allows the evaluation of the coupling between inner modes and free space modes, which is equivalent to the energy transfer between inside and outside the PBG. The treatment and visualization data are realized with MATLAB software [14].

The FDTD technique is a simple and efficient method to solve the differential equations. It solves the discretized Maxwell's equations in the time domain and evaluates the EM field components (e_x, e_y, e_z, h_x, h_y, h_z) in each cell of a gridding computational volume.

The method used to obtain the propagation modes inside the metallic PBG is essentially based on the Fourier transform of the EM fields in time and space domain (Figure 14).

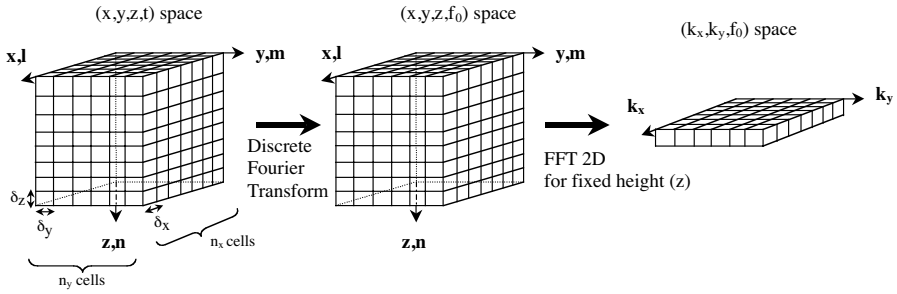

Figure 14. Method of calculation.

FDTD method gives the value of each electromagnetic component (e_x, e_y, e_z, h_x, h_y, h_z) in a discrete time and space domain. A Fourier transform is then applied on the field components to go from the time domain to the frequency domain. The field components in the frequency domain (at f_0 frequency chosen by the user) are obtained with a discrete Fourier transform realized during the time iteration of the FDTD computation. This avoids the storage of all the field

components in the time domain.

$$e_{x_{f_0}}(x,y) = \sum_t e_x(x,y,t)\cdot \exp^{(-j2\pi f_0 t)} \quad (2a)$$

$$e_{y_{f_0}}(x,y) = \sum_t e_y(x,y,t)\cdot \exp^{(-j2\pi f_0 t)} \quad (2b)$$

$$e_{z_{f_0}}(x,y) = \sum_t e_z(x,y,t)\cdot \exp^{(-j2\pi f_0 t)} \quad (2c)$$

Where x and y are the components of the real space, t is the time variable and f_0 the frequency for which the Fourier transform is computed. We have the same equations for the magnetic field H and its components.

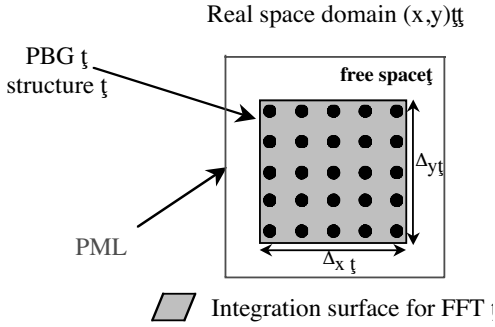

Figure 15. Area to apply FFT 2D.

Finally, a bidimensional Fourier transform is performed on the space coordinates inside the surface area shown in Figure 15 to obtain the distribution of the modes in the reciprocal space.

$$e_{x_{f_0}}(k_x,k_y) = \sum_l \sum_m e_{x_{f_0}}(l,m)\cdot \exp^{j(k_x l\delta x + k_y m\delta y)} \quad (3a)$$

$$e_{y_{f_0}}(k_x,k_y) = \sum_l \sum_m e_{y_{f_0}}(l,m)\cdot \exp^{j(k_x l\delta x + k_y m\delta y)} \quad (3b)$$

$$e_{z_{f_0}}(k_x,k_y) = \sum_l \sum_m e_{z_{f_0}}(l,m)\cdot \exp^{j(k_x l\delta x + k_y m\delta y)} \quad (3c)$$

Where k_x and k_y are the coordinates in the reciprocal space. Because of the structure meshing, the components are evaluated thanks to the discrete coordinates l and m of the real space. δx and δy are the spatial steps of meshing in the real space. During the calculation, each component is stored in a matrix whose number of elements is equal to the product of n_x by n_y (number of cells in the x and y directions).

In the simulation, the structure is surrounded by PML (Perfectly Matched Layer) absorbing boundaries to replace the free space. In order to excite all the propagation XY-plane directions inside the PBG, two kinds of excitation can be used: the current line or the radiating localize element. We will pay our attention on a current line source whose main advantage is to reduce the computation volume thanks to the boundary condition. Some examples are given in [15, 16] with a dipole excitation.

In the reciprocal space, the distribution of the different EM field components and the power density at the f_0 frequency can be observed versus the real value of the wave vector components (k_x and k_y).

2.3. Some Results

All the structures that we will consider have a 12 mm period and a 0.2 mm diameter (Figure 16). Only the number of layers is different (4 or 8).

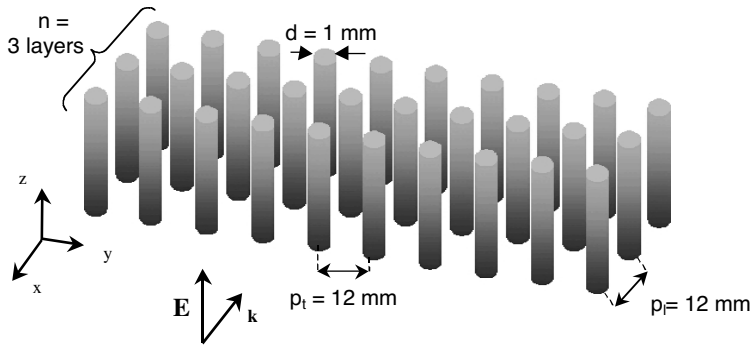

Figure 16. Metallic PBG structure excited with a plane wave excitation.

First of all, we present the reflection coefficients of these structures, when excited with a normal incidence plane wave Section 2.3.1. Then, we present the propagation modes inside the MPBG structures excited with an infinite current line Section 2.3.2.

2.3.1. Plane Wave Excitation

Let us consider the structure described in Figure 16 excited with a normal incidence plane wave. This structure is supposed infinite according to the y and z direction. In the simulation software, infinite periodic structures are realized using PEC (Perfect Electric Conductor) and PMC (Perfect Magnetic Conductor) boundary conditions.

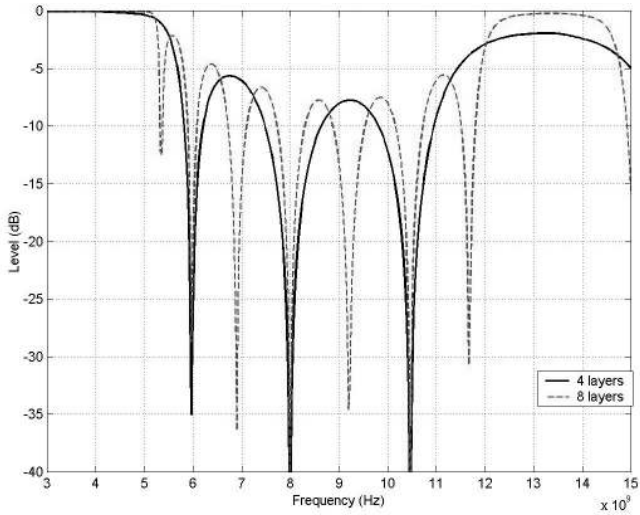

Figure 17. Theoretical reflection coefficients for two metallic PBG structures (4 or 8 layers) with period = 12 mm and diameter = 0.2 mm.

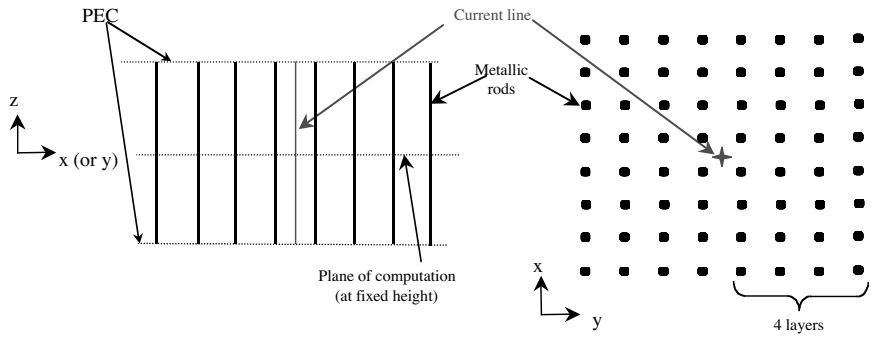

Figure 18. Current line location inside the structure.

Table 5. Propagation peaks for two metallic PBG structures (4 or 8 layers.

Frequency (GHz)	5.35	**6.0**	6.9	**8.0**	9.2	**10.5**	11.7
4 layers		**1st peak**		**2nd peak**		**3rd peak**	
8 layers	1st peak	**2nd peak**	3rd peak	**4th peak**	5th peak	**6th peak**	7th peak

The black outline describes the Brillouin zone limitation $(in \pm \frac{\pi p_l}{2} et \pm \frac{\pi p_t}{2})$.

Propagationţ Frequencyţ	*4 layers structureţ*	*8 layers structureţ*
1ţtpeakţ	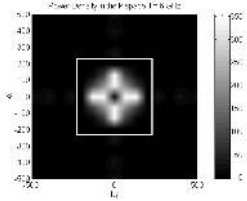 f = 6 GHzţ	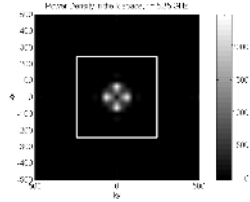 f = 5.35 GHzţ
2ţdtpeakţ	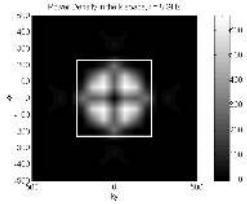 f = 8GHzţ	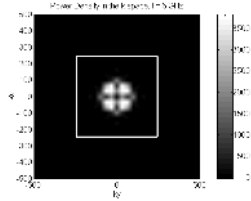 f = 6GHzţ
3ţdt peakţ	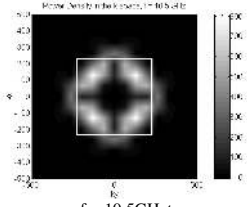 f = 10.5GHzţ	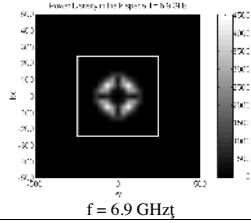 f = 6.9 GHzţ
4ţhtpeakţ		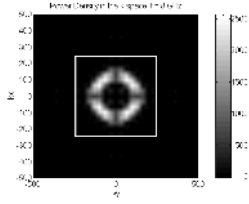 f = 8 GHzţ
5ţhtpeakţ		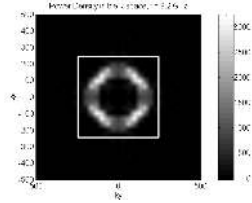 f = 9.2 GHzţ

Figure 19. Power density in the reciprocal space for two different structures (Figure 16) at several propagation frequencies.

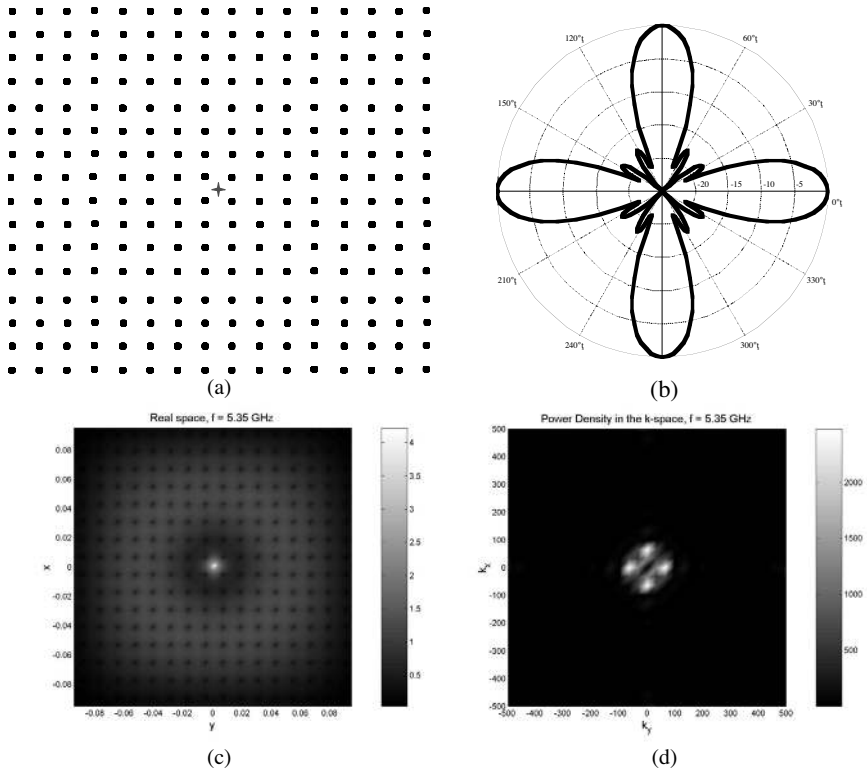

Figure 20. Results for a 8 layers metallic PBG structure at 1st propagation peak (5, 35 GHz).
(a) Top view of the structure.
(b) Radiation pattern ($\theta = 90°$, $0 < \varphi < 360°$).
(c) Energy repartition in the real space.
(d) Power density in the reciprocal space.

The reflection coefficients are represented in Figure 17 for two structures (4 or 8 layers). They both exhibit a band-gap between the zero frequency and 5 GHz, then a propagation band with different propagation peaks. We can see these structures have common peaks at 6, 8 and 10.5 GHz. These peaks are listed in the Table 5.

For each propagation peak corresponds a propagation mode with a particular repartition of energy inside the structure and particular possible directions of propagation.

We will then present the power density at these propagation peaks, computed with the FDTD algorithm.

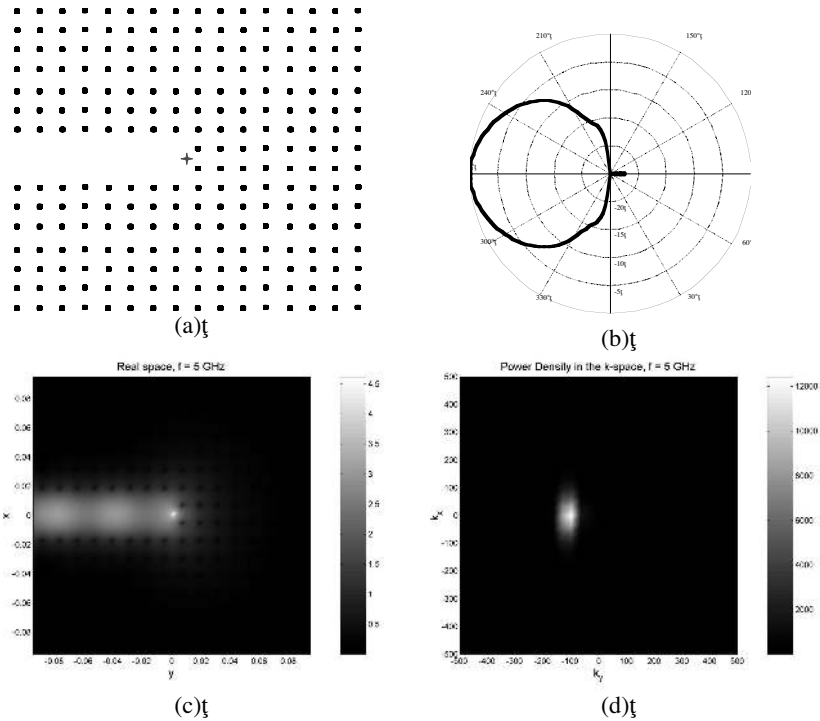

Figure 21. Results for a 8 layers metallic PBG structure with a linear defect.
(a) Top view of the structure.
(b) Radiation pattern ($\theta = 90°,\ 0 < \varphi < 360°$).
(c) Energy repartition in the real space.
(d) Power density in the reciprocal space.

2.3.2. Infinite Current Line

Complete structures analysis

An infinite current line located in the middle of the structure (Figure 18) is used to visualize the propagation modes in the XY-plane.

The FDTD method allows the visualization of the power density inside a finite Metallic PBG structure at different frequencies (Figure 19). We compare two structures which have a different number of layers (4 or 8). We can observe in Figure 19 that the power density is the same for the same propagation mode (i^{th} peak) of each structure. On the other hand, if we compare two mode diagrams at the same

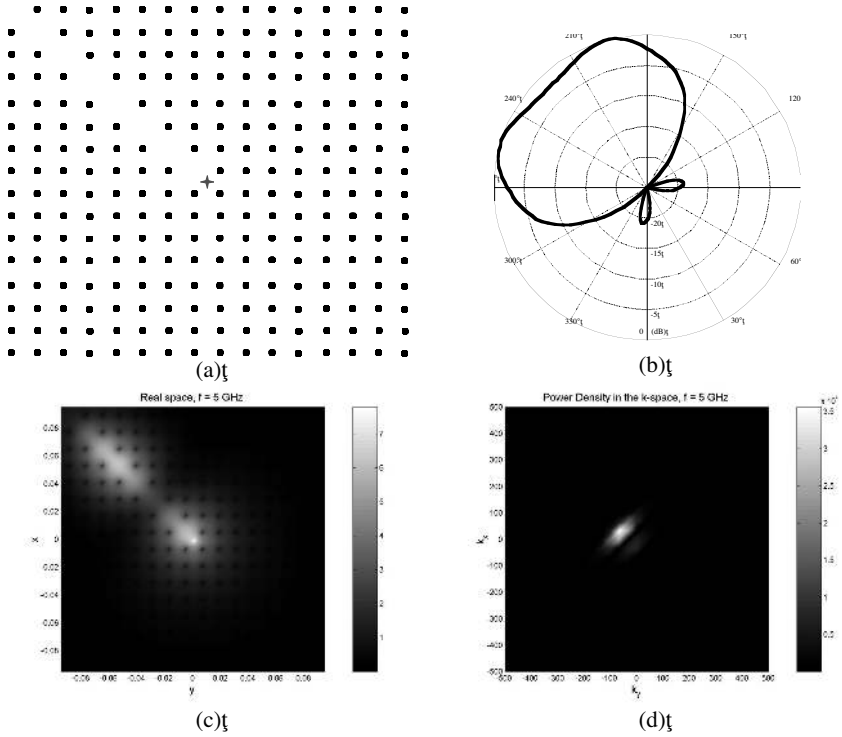

Figure 22. Results for a 8 layers metallic PBG strcuture with a "diagonal" linear defect.
(a) Top view of the structure.
(b) Radiation pattern ($\theta = 90°, 0 < \varphi < 360°$).
(c) Energy repartition in the real space.
(d) Power density in the reciprocal space.

frequency, we can notice they are not the same. The reason is that frequencies associated to propagation modes are different.

An example of a 8 layers structure is presented in Figure 20(a). Figure 20 presents a good correlation between the directions of the radiated far field beams (Figure 20(b)) and the direction of propagation modes inside the MPBG (Figure 20(d)).

Structures with defects

Now, let us consider the metallic PBG structures with defects (suppression or addition of metallic wires). Defect modes inside PBG are very important as they produce a very particular radiation pattern.

Let us consider the metallic PBG structure with a linear defect represented in Figure 21(a). This kind of defect creates a wave guide in the MPBG structure. The dipole is excited at a frequency inside the band-gap of the MPBG without defects and larger than the cut-frequency of the equivalent wave-guide. The radiation pattern is given in the Figure 21(b) and with the energy distribution in the real space in the Figure 21(c).

Most of the energy is radiated along the linear defect. The propagation mode diagram — Figure 21(d) — is well correlated with the radiation pattern and the energy density in the xy-plane. The radiation pattern exhibits a large lobe in the direction of defect. In this case, a lot of propagation modes are excited to obtain a large lob. The mode diagram shows that a set of modes are excited due to the relatively large mode density. The mode diagram demonstrates very well the directions of propagation. This method can be performed to more complex structures like the 3D dimensional metallic PBG or the mixed PBG.

As we can see, this approach gives a complete information about the propagation inside the MPBG with defects.

3. CONCLUSION

A commercial Finite Element Method (FEM) package, with the release of ANSOFT HFSS 7 and its associated OPTIMETRICS Engine, was used to achieve a parametrical study of a metallic PBG structure with continuous or discontinuous wires in the X-Band (8–12 GHz).

Through this study, it has been shown the well-known relationships about continuous structures:

- When the period (longitudinal or transversal) increases, stop band and propagation band shift in lower frequencies.
- When the diameter increases, stop band and propagation band shift in higher frequencies.
- They are $(n-1)$ propagation peaks for a n layers structure (under normal incidence).

Moreover it has been shown the influence of each parameter on the bandwidth (of stop band or propagation band) and also on transmission coefficient level. Thus, if a PBG structure is required in propagation band, a low longitudinal period, a high transverse period and a thin diameter are suitable.

Concerning the PBG structure with discontinuous wires, the propagation bandwidth increases when the axial period decreases and the spacing enlarges.

In the other section, a numerical method based on the FDTD method and the Fourier transform is presented. This one gives more information than others methods to analyze the complex metallic PBG with or without defects in two or three dimensions, and this under real conditions (type of excitation, finite size of the structure,. . .).

It can be shown that with applying the numerical method (the FDTD method and the Fourier transform) on MPBG structures a good performance is obtained. The first advantage of the applied method is that the technique exhibits the reduction of surface waves by the metallic PBG. This reduction is important to enhance the radiated power and to obtain a better shape of the beam. The use of MPBG allows to obtain a better reduction of energy distribution in the undesirable way. Moreover, this method allows to analyze the behavior of EM waves in the complex metallic PBG with defects under real condition.

ACKNOWLEDGMENT

The authors would like to acknowledge Professor C. Terret and P. Pouliguen for their help.

REFERENCES

1. Yablonovitch, E., "Photonic band-gap structures," *J. Opt. Soc. Amer. B, Opt. Phys.*, Vol. 10, 283–295, February 1993.
2. Joannopoulos, J. D., R. D. Meade, and J. N. Winn, *Photonic Crystals*, Princeton Univ. Press, Princeton, NJ, 1995.
3. Zhang, Z. and S. Satpathy, "Electromagnetic waves in periodic structures: Bloch wave solution of Maxwell's equations," *Physical Review Letters*, Vol. 65, 2650, 1990.
4. Marcuvitz, N., *Waveguide Handbook*, MacGraw Hill Book Company, 1951.
5. Ansoft-HFSS (High Frequency Structure Simulator), Vol. 7, Commercial 3D finite-element package.
6. Ho, K. M, C. T. Chan, and C. M. Soukoulis, "Existence of a photonic gap in periodic dielectric structures," *Phys. Rev. Lett.*, Vol. 65, 3152, 1990.
7. Ozbay., E. et al., "Measurement of a three-dimensional photonic band gap in a crystal structure made of dielectric rods," *Phys. Rev.*, B 50, 1945, 1994.
8. Poilasne, G., P. Pouliguen, K. Mahdjoubi, L. Desclos, and C. Terret, "Active metallic photonic band-gap materials (MPBG):

Experimental results on beam shaper," *IEEE Transaction on Antennas and Propagation*, Vol. 48, 117–119, January 2000.

9. De Lustrac, A., F. Gadot, S. Cabaret, J. M. Lourtioz, T. Brillat, A. Priou, and E. Akmansoy, "Experimental demonstration of electrically controllable photonic crystals at centimeter wavelengths," *Applied Physical Letters*, Vol. 75, 1625–1627, September 1999.
10. Taflove, A. and M. E. Brodwin, "Numerical solution of steady state electromagnetic scattering problems using the time-domain dependent Maxwell's equations," *IEEE Microwave Theory and Techniques*, Vol. 23, No. 8, August 1975.
11. Taflove, A., *Advances in Computational Electrodynamics, the Finite-Difference Time-Domain Method*, Artech House.
12. Thévenot, M., A. Reinex, and B. Jecko, "FDTD to analyze complex PBG structures in the reciprocal space," *Microwave and Optical Technology Letters*, Vol. 21, No. 1, April 1999.
13. Guiffaut, C., FDTD Code Developed in RENNES.
14. MATLAB edited by The Mathworks Inc., Computation, Visualization and Programming Package.
15. Collardey, S., G. Poilasne, A.-C. Tarot, P. Pouliguen, K. Mahdjoubi, and C. Terret, "Metallic photonic band-gap propagation modes characterization," *Microwave and Optical Technology Letters*, March 2001.
16. Collardey, S., G. Poilasne, A.-C. Tarot, P. Pouliguen, K. Mahdjoubi, and C. Terret, "Propagation modes in k-space and radiation pattern of metallic photonic band gap materials," ISAP2000, Fukuoka, Japan, August 21–25, 2000.